

ISSN: 2523-5672 (Online)

Water Conservation & Management (WCM)

DOI: http://doi.org/10.26480/wcm.02.2025.346.355



CODEN: WCMABD

RESEARCH ARTICLE

FLOOD HAZARD MODELING USING GIS AND IBER TOOLS: AN INTEGRATED APPROACH

Hanane Azour^a, Mohamed Mansoum^a, Hicham Sabar^b, Yassine EL Yousfi^c, Imane Ammar^d, Hicham Gueddari^e, Mohamed Benmakhlouf^f, Iamal Mabroukig^e

- aGeomorphology, Environment and Society Laboratory, Department of Geography, Faculty of Letters and Human Sciences, Cadi Ayyad University,
- ^bLaboratory of Geoscience Applique, University Mohamed First Oujda.
- ^cLaboratory of Applied Sciences, Environmental Management and Civil Engineering, GEGC, ENSAH, Abdelmalek Essaadi University, Tetouan, Morocco.
- ⁴Applied Geosciences Laboratory Geology Department Faculty of Science Université Mohammed premier.
- ^eLaboratory OLMAN-BPGE, Multidisciplinary Faculty of Nador, Mohamed First University, Oujda, 62700 Nador, Morroco.
- ${\it Laboratory of Applied and Marine Geosciences, Geotechnics and Geohazards, Abdelmalek Essaadi University, Tetouan, Moroccontrol of Control of Control$
- g Laboratory of Spectroscopy, Molecular Modeling, Materials, Nanomaterial's, Water and Environment, CERNE2D, Mohammed V University in Rabat, Faculty of Science, AV Ibn Battouta, BP1014, Agdal, Rabat, Morocco
- *Corresponding Author Email: jamal.mabrouki@um5s.net.ma

This is an open access journal distributed under the Creative Commons Attribution License CC BY 4.0, which permits unrestricted use, distribution, and reproduction in any medium, provided the original work is properly cited

Article History:

Received 05 March 2025 Revised 12 April 2025 Accepted 28 April 2025 Available online 23 May 2025

ABSTRACT

This study focuses on flood risk assessment in the Al Hoceima region, utilizing advanced modeling tools such as IBER and HEC-HMS to develop comprehensive flood maps. A detailed digital terrain model (DTM) was processed alongside land use classifications derived from high-resolution satellite imagery, which identified five key land use categories: built-up areas, dense vegetation, forests, infrastructure, and transitional zones. The hydrological simulation revealed varying flood discharge characteristics across three watersheds, with maximum flow rates reaching 80 m³/s in highly urbanized areas. Flood maps classified regions into low, medium, and high-risk categories based on water depth and flow velocity, highlighting significant vulnerabilities in densely populated sectors. The results indicate that 75% of flood events occurred between November and February, aligning with peak precipitation periods. Suggested actions include enhancing drainage infrastructure, regulating urban development in high-risk zones, and implementing community awareness programs. Overall, this research provides vital insights for effective flood risk management, aiding local authorities in making informed decisions to safeguard the population and infrastructure.

KEYWORDS

Flood Risk Assessment, Hydrological Simulation, Digital Terrain Model (DTM), Urbanization, Al Hoceima Flood Mapping.

1. Introduction

Global climate circulation models forecast more severe weather and precipitation events than those recorded. The impacts of climate change are more evident in developing nations, especially in people situated in vulnerable regions (Gaudiano, G., 2007; Valentín et al., 2022; Res and Trenberth, 2011; Valentín et al., 2022). Currently, our planet is encountering an unprecedented frequency of natural disasters (Case and Bayadh, 2023; Vignesh, 2021). This may result in various harms that jeopardize human life and the environment(Afzal et al., 2022; Sami et al., 2021), impacting millions of individuals each year (Afzal et al., 2022; Alfieri et al., 2018) and resulting in more casualties than other catastrophic natural events globally (ARDC, 2009; IRFC, 2003).

The flood risk is widely recognized as one of the most destructive natural hazards on a global, national, regional, and local scale (Afzal et al., 2022; Ashley and Ashley, 2008). Recent flood disasters worldwide demonstrate that the severe consequences of urban floods often coincide with high population densities and related developments in urban regions

(Nkwunonwo et al., 2018). The rapid expansion in global population and the accumulation of wealth result in heightened human vulnerability, with additional personal and corporate wealth at greater danger(Nkwunonwo et al., 2018). The flood phenomena are triggered by a combination of factors, including overflowing rivers, excessive water accumulation following intense precipitation, snowmelt, marine storms, and, in some cases, the failure of hydraulic infrastructures such as dams. These events can occur suddenly and unpredictably, or develop gradually, taking various forms, such as flash floods in mountainous or urban areas, and more extensive and prolonged flooding in river plains.

The severity of flooding is often intensified by topographical factors, such as slope, soil composition, saturation, and anthropogenic factors, including unplanned urbanization, deforestation, and poor watershed management. These factors can intensify water flows, reduce the soil's natural absorption capacity, and amplify the impact. The consequences of flooding are often catastrophic, not only in terms of loss of life, but also in terms of destruction of material assets, disruption of critical infrastructure, and the resulting social and economic disruptions. Flood control measures are

Quick Response Code Access this article online



Website: www.watconman.org DOI:

10.26480/wcm.02.2025.346.355

categorized into structural and nonstructural types. The aim of the former is to mitigate or diminish the destruction inflicted by a flood, via the establishment of meticulously planned and engineered structures. The latter pertains to the preparation, organization, coordination, and implementation of a series of Civil Protection exercises aimed at preventing or mitigating flood-related damage (Salas Salinas, 2014).

Historically, Morocco has been marked by many significant floods, which testify to the country's vulnerability to these natural phenomena. Due to its varied geography, ranging from vast coastal plains to the rugged Atlas and Rif mountains, combined with a semi-arid climate, Morocco presents conditions conducive to flooding, particularly during periods of heavy rainfall. Floods in regions such as Marrakech, Agadir and the Rif have become recurrent events, caused significant damage and highlighted the need to improve risk management strategies. The World Bank research (2011) titled "Climate Change Adaptation and Resilience to Natural Disasters in Coastal Cities of North Africa" indicated that a temperature increase of 4°C would impact 2.1 million individuals in Morocco due to flooding (Satta, et al., 2023). The imminent threat of sea level rise in the forthcoming decades is exacerbated by the dense population and activities in coastal regions, alongside heightened threats from rising global sea levels, intensified storms, and localized coastal erosion. The World Bank has classified Morocco's coastal GDP among the Top 10 nations at risk of escalating storm surges (Dasgupta et al., 2023).

The Al Hoceima region, in particular, is a good illustration of the challenges posed by flooding in Morocco. This area, characterized by rugged terrain, irregular rainfall and a complex hydrological network, is particularly vulnerable to torrential flooding. Flooding is often the result of intense rainfall that exceeds the infiltration capacity of the soil, causing rapid surface runoff and sudden flooding. The region's inadequate drainage infrastructure also accentuates the risks.

Notable events included the flooding in February 2017, impacted severely on the city of Al Hoceima. This flood, caused by unusually heavy rainfall, highlighted the limitations of existing urban drainage systems, resulting in major flooding that caused considerable material damage, particularly to homes and commercial infrastructure. Similarly, in March 2008, torrential flooding isolated villages in Beni Boufrah, emphasizing the vulnerability of rural areas where access to emergency services is limited.

In November 2012, the town of Imzouren was submerged by flooding of Oued Nekor, an event that highlighted the need for more rigorous watershed management and early warning systems. The January 2015 floods in the Tamasint valley were also associated with land movements, increasing the risks for local populations and requiring emergency interventions to avoid loss of life. Finally, in October 2019, flash floods hit Bni Bouayach, illustrating once again the vulnerability of rural infrastructures to climatic hazards.

These events underline the urgent need for an integrated approach to water management and infrastructure improvement in the Al Hoceima region. It is essential to strengthen local capacities for flood prevention and response, through the implementation of early warning systems, improved drainage infrastructures, and urban planning adapted to hydrological risks. In addition, a thorough understanding of the underlying causes and consequences of flooding is crucial to developing effective mitigation strategies. This includes a detailed analysis of climate patterns, local hydrological characteristics and the socio-economic factors that influence populations vulnerability.

Iber was created by integrating two pre-existing two-dimensional numerical modeling tools, Turbillon and CARPA (Bladé et al., 2014; Bladé et al., 2008; Cea and Puertas, 2007) both employing the finite volume method, into a singular, enhanced code with additional functionalities. The Iber model comprises various interconnected computing components.

The main objective of this study is to draw up an accurate and detailed map of flood risk areas in Al Hoceima, by implementing an appropriate methodology, collecting the required information, using IBER and HMS HEC software to represent the flood risk, and creating a reliable and usable map for decision-making purposes.

In conclusion, flooding in the Al Hoceima region represents a major challenge requiring sustained attention and coordinated action at all levels of society. Improving resilience to flooding requires concerted efforts in water resource management, urban planning and raising community awareness of hydrological risks. The impact of flooding on people and infrastructure is considerable. Accurate flood hazard mapping is therefore crucial to better risk management and urban planning.

Developing sustainable solutions to reduce the impact of flooding is not only a priority for the safety of populations, but also for the region's long-term economic and social development.

2. MORPHOMETRIC CHARACTERISTICS OF THE AL HOCEIMA WATERSHED

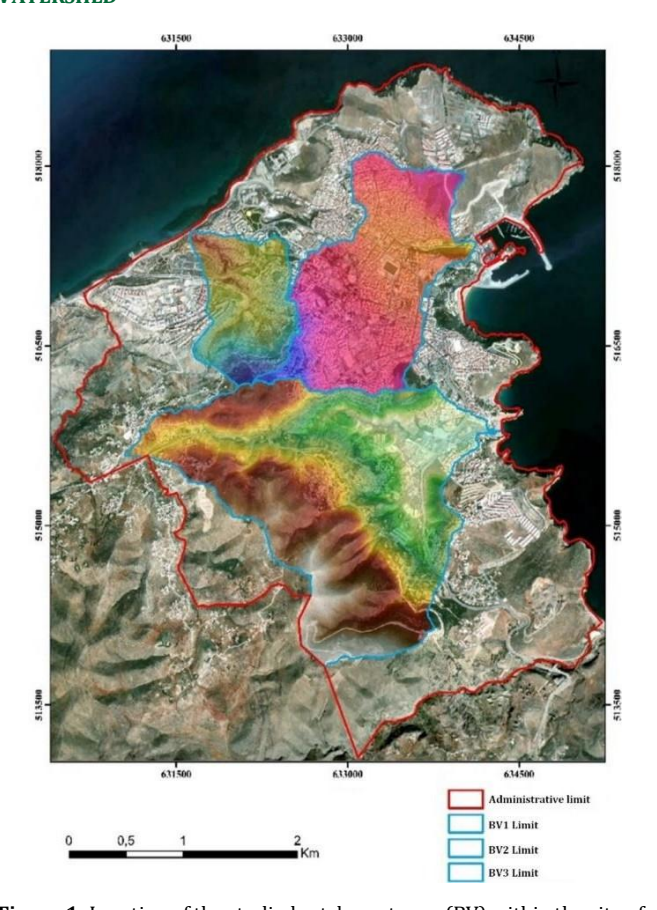


Figure 1: Location of the studied catchment area (BV) within the city of Al Hoceima

Al Hoceima is a coastal city in the Tangier-Tetouan-Al Hoceima region of northern Morocco. It is surrounded by the Rif mountains and has a coastline on the Mediterranean Sea. The city's complex topography, combined with heavy rainfall in certain seasons, places it at high risk of flooding. This presentation of the city will provide a better understanding of the issues related to flooding and help define the most vulnerable areas. In our study area, watersheds are located either in the center of a city, or in developed areas, a particularly complex configuration due to the interaction between natural hydrological processes and urban infrastructures. In this situation, the urban area is directly exposed to the risk of flooding. The areas where the various watercourses meet, such as Ouaraa El Quodes or Mirador Bas, are particularly vulnerable due to uncontrolled urban expansion. This has led to an increase in soil impermeability and a reduction in natural hydrological absorption and retention capacities.

For this reason, the surface area and shape of catchment areas significantly influence the hydrological response of rivers at their outlets. It is therefore crucial to carry out a study of the morphometric characteristics of the catchment areas of the city of Al Hoceima, given the diversity of sizes and shapes that these areas present.

The following morphometric characteristics influence the hydrological behavior of a watershed. Figure 1 shows that BV1 is the largest, with a surface area of 4.12 km, followed by BV2 with a surface area of 8.06 km and finally BV 3 with a surface area of 4.33 km. BV2 is totally located in the center of the city of al Hoceima, which can create a real flood risk.

2.1 Watershed's terrain model

The development of a watershed terrain model depends on the accuracy of the digital terrain model (DTM), which is used to delimit the watershed and divide it into sub-watersheds, each with its own flow axis. The reliability of the results depends on the accuracy of the DTM, hence the importance of this operation. In our case, we began by using the DTM used by the urban

agency as part of a contract to produce a constructibility map with a resolution of 30 meters. This resolution is sufficient to build the watershed model. The model is prepared and pre-processed on arcgis 10.8 as follows:

- Fill: Hydrologically correct DTM (no depressions due to interpolation).
- · Fdr: Flow direction.
- Fac: Flow accumulation.
- Str: Stream definition.
- StrLnk: Stream segmentation.
- Cat: Catchment grid delineation (one catchment area for each flow axis).
- Catchment: (vectorization of watershed raster).
- DrainageLine: Drainage line processing.
- Adjoint Catchment: Watershed aggregation.

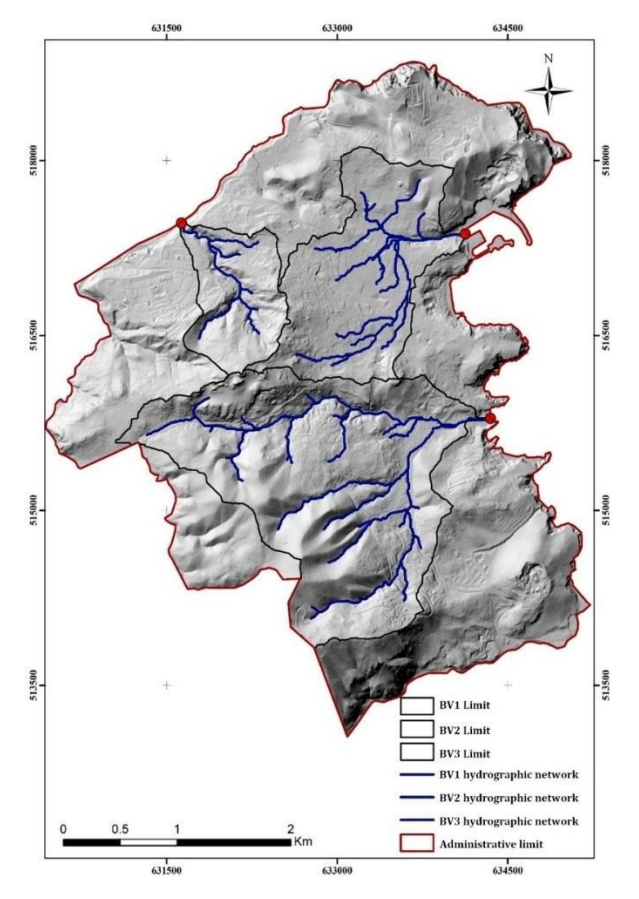


Figure 2: Watershed model based on DTM

3. GRAVELIUS COMPACTNESS INDEX (KC)

Graveluis index is one of the fundamental concepts in urbanisme field which determine the compactness of the watersheds. The analysis states that hydrologists utilize Gravilius's compactness index (Hassani et al., 2021; Roche, 1963)

These latter offer insights on the watershed's morphology, significantly affecting the entire flow of the watercourse and particularly the configuration of the hydrograph at the basin's exit, resulting from a specific precipitation event(Ouzerbane et al., 2019). Generally this index represents the ratio between the aera of the watershed A and its perimeter P.

The coefficient is defined as follows:

$$k_c = 0.28 \times \frac{P}{c^{1/4}}$$

Where P = watershed perimeter (km) and A = area (km²).

A high Kc value indicates a more compact and efficient soil. On the other hand, a low Kc value indicates a more dispersed, less efficient layout.

Table 1: Correspondence between Kc value and type of hydrological response expected (LASRI, 2014)

Index Shape		Respond		
Kc < 1,25	Compact watershed	Fast respond		
1,25< Kc < 1,5	Medium watershed	Medium respond		
Kc > 1,5	Extended watershed	Slower respond		

Table 2: Kc calculation for each BV			
BV	Perimeter	Area	Kc
1	10.53	4.12	1.45
2	8.06	2.02	1.59
3	4.33	0.89	1.29

Table $N^{\circ}2$ shows that the Kc values are slightly different for the three basins, basin 2 being the highest (1.59), basin 1 (1.45) and basin 3 the lowest (1.29), which means that basin 2 has the greatest capacity to delay the flow of water towards its outlet due to its elongated shape, while basin 3 has the quickest response due to its rounded shape, which can give us a floodable area.

3.1 Estimation of the time of concentration of flood in the Al Hoceima agglomeration.

Comprehending a watershed's response to rainfall events is crucial for numerous hydrological and hydraulic studies, including water resource management, irrigation, hydraulic infrastructure design, and flood control planning (Costabile et al., 2024).

Generally, floods are the most predictable, as their occurrence is often linked to a well-defined hydro-climatic process. This relationship makes it possible to anticipate their occurrence and, consequently, to trigger warnings aimed at minimizing potential damage. However, flood forecasting is not always sufficient to effectively warn riverside populations and protect their property, due to the flood concentration time, which can be very short.

Time of concentration is defined as the time required for runoff water generated by precipitation to cross the entire watershed and reach its outlet, generally identified by the main outlet. More precisely, this is the time interval between the start of precipitation and the moment when maximum flow is observed at the watershed outlet. Since the 1920s, numerous academics have formulated empirical equations to predict Tc for ungauged catchments of diverse sizes and physiographies (Perdikaris et al., 2018). This parameter is crucial for hydrological assessment, as it directly influences the response of the watershed to precipitation, and consequently, flood forecasting. Five empirical formulas are used to calculate this parameter:

The five formulas are presented below:

- Kirpich: Tc = 32.5.10-5 * L 0.77 * I -0.385 with:
 - o Tc: time of concentration in hours
 - o L: length of longest thalweg in m
 - o I: average slope in m/m
- Espagnol: $Tc = 60 \times 0.30 \times (L/P^{0.25})^{0.77}$ with:
 - o Tc: time of concentration in minutes
 - o L: length of the principal wtercurse in km.
 - I: average slope in m/m
- Californienne: $Tc = 0.019395 \times (\frac{L}{p^{1/2}})^{0.7}$ with:
 - $\circ \qquad \text{Tc: time of concentration in minutes} \\$
 - L: length of longest thalweg in m
 - o P: slope in m/m.
- Ventura: $Tc = 76.3 \times (L/P)^{0.25}$ with:
 - o Tc: time of concentration in minutes

- o L: length of longest thalweg in km
- o P: slope of the catchment watershed in m/m.
- Turazza: $Tc = 60 \times 0.108 \times (S \times L)^{0.333} \times P^{0.5}$ with:

- Tc: time of concentration in minutes
- S: Area of the catchment watershed in km²
- L: distance in km between the outlet and the furthest point of the watershed
- o P: average slope in m/m

Table 3: time of concentration calculation by type for each basin						
Oueds / calculation	Time of concentration calculated using various empirical formulas (h : min)					
point (city entrance / dams or outlet)	Kirpich	Californienne	Espagnol	Turraza	Ventura	Adopté
BV I	19.76	43.25	60.43	40.87	42.77	41.42
BV II	10.25	22.42	31.76	24.09	29.63	23.63
BV III	11.875	10.94	23.93	32.81	19.64	20.89

3.2 Determination of coefficients a and b

The coefficients a and b are obtained by adjusting rainfall data recorded over an extended period at a station. They are used to create IDF curves, which combine rainfall data for various return periods (Elhaddaji, 2019). It is essential to use Montana coefficients to apply certain method-related formulas, such as the rational, mac math and Burklier_Ziegler methods to determine the peak discharge of a flood from these empirical methods. The montana coefficients used in our study are obtained from the report (Direction of roads, 2015).

3.3 Determination of flow rates using empirical methods

- BVI: The rational method indicates a peak flow of 0.57 m3/s for watershed I, while the Burklier-Ziegler method indicates a slightly lower flow of 0.49 m3/s. In this watershed, there is no value for the MacMath method. The two methods (Rational and Burklier-Ziegler) show a relatively small difference of around 14%. This may be linked to the way in which each method takes into account parameters such as slope, basin surface and precipitation. The values obtained by the rational method are generally higher, as it is based on simple empirical formulas.
- BVII: The rational method calculates a peak flow of 0.40 m3/s, while
 the Burklier-Ziegler method estimates a peak flow of 0.30 m3/s. As
 in the case of BV I, there are no data available for the MacMath
 method here. There is a more significant disparity (25%) between
 the two methods. This can be attributed to the disparities in the
 consideration of hydrological elements (runoff, rainfall) between
 these different methods.
- BVIII: The rational method gives a peak flow of 0.18 m3/s for BV III, which is similar to the result obtained by the Burklier-Ziegler method (0.19 m3/s). The MacMath method, which is used in this situation, provides a significantly lower flow of 0.02 m3/s. In summary, the MacMath method generates a significantly lower flow than the other methods for this catchment watershed. This may be due to specific assumptions or parameters employed in this method, which differ from the others, particularly in the way precipitation and watershed shape are taken into account.

Table 4: Montagna coefficient values for each return period				
DV	Flow			
BV	Rationnal	Mac math	Burklier_Ziegler	
BV I	0.57	-	0.49	
BV II	0.40	-	0.30	
BV III	0.18	0.02	0.19	

Table 5: Empirical Data of Coefficients a and b as a Function of T			
T	a	b	
10	4.172	0.570	
50	5.606	0.562	
100	6.215	0.560	

4. RESEARCH METHODOLOGY

This study aims to produce a flood risk map for the city of Al Hoceima, using IBER and arcgis10.8 software. In this case, a rigorous methodological

approach will be adapted, The simulations concentrate on a return period of T=100 years and are conducted in multiple phases (Adil et al., 2024).which will include the collection of topographic, hydrological and meteorological data, as well as the implementation of IBER software for modeling.

Flood hazard modelling methods include the use of specialist software such as IBER, which assesses flood risk by integrating hydrological, hydraulic and topographical data to simulate flood scenarios. IBER is well known for its ability to simulate river flows and coastal flooding. This software is used to analyze hydraulic and hydrological processes, taking into account topographical features and meteorological data. The combination of the two enables comprehensive flood hazard modeling, making it a valuable tool in our study.

The data used To complete the flood hazard map for the city of Al Hoceima, it is essential to collect accurate and reliable data. This includes topographical, hydrological and meteorological data, as well as information on land use. Data will be collected from government sources, local weather stations, field surveys, satellite imagery and ecognition software. Data reliability is crucial to ensure accurate modeling and flood hazard mapping.

The Iber model, set up to simulate water flows, gives us reliable hydraulic scenarios for dealing with difficult and complicated hydraulic situations, such as surface runoff, urban flooding and wet drought interfaces. Accurate modeling of hydrostatic and dynamic forces is ensured by the shallow water equations integrated into Iber, especially under conditions where surface elevation plays an important factor. One of Iber's strengths is its ability to efficiently balance the conservation of mass and momentum equations, even in irregular terrain and during wet-dry transitions (Mediero et al., 2022).

Soto and Malpartida stated that Iber uses a two-dimensional mathematical model that offers advantages over one-dimensional models in terms of improved stability and accuracy for reliable results (Gomes, 2018; Soto and Malpartida, 2016). In fact, it is able to simulate water flow more realistically in all situations where water flow is not solely unidirectional.

The processes integrated in Iber are based on the hydrodynamic module, which solves the two-dimensional shallow water equations, also known as the 2D Saint-Venant equations (Figure 2). These are divided into three equations: the first is the continuity equation, the other two describe the conservation of momentum in water (Gomes, 2018; Jean et al., 2010; Mediero et al., 2022).

$$\frac{\partial h}{\partial t} + \frac{\partial hU_x}{\partial x} + \frac{\partial hU_y}{\partial y} = 0$$

$$\frac{\partial}{\partial t} (hU_x) + \frac{\partial}{\partial x} (hU_x^2 + g \frac{h^2}{x}) + \frac{\partial}{\partial y} (hU_x^U) = -gh \frac{\partial z_b}{\partial x} + \frac{\tau_{s,x}}{\rho} - \frac{\tau_{b,x}}{\rho} + \frac{\partial}{\partial y} (v_t h \frac{\partial U_y^2}{\partial x}) + \frac{\partial}{\partial y} (v_t h \frac{\partial U_y^2}{\partial y}) = -gh \frac{\partial z_b}{\partial x} + \frac{\tau_{s,x}}{\rho} - \frac{\tau_{b,x}}{\rho} + \frac{\partial}{\partial y} (v_t h \frac{\partial U_y^2}{\partial y}) = -gh \frac{\partial z_b}{\partial x} + \frac{\tau_{s,x}}{\rho} - \frac{\tau_{b,x}}{\rho} + \frac{\partial}{\partial y} (v_t h \frac{\partial U_y^2}{\partial y}) = -gh \frac{\partial z_b}{\partial x} + \frac{\partial}{\rho} (v_t h \frac{\partial U_y^2}{\partial y}) = -gh \frac{\partial z_b}{\partial x} + \frac{\partial}{\rho} (v_t h \frac{\partial U_y^2}{\partial y}) = -gh \frac{\partial z_b}{\partial x} + \frac{\partial}{\rho} (v_t h \frac{\partial U_y^2}{\partial y}) = -gh \frac{\partial z_b}{\partial x} + \frac{\partial}{\rho} (v_t h \frac{\partial U_y^2}{\partial y}) = -gh \frac{\partial z_b}{\partial x} + \frac{\partial}{\rho} (v_t h \frac{\partial U_y^2}{\partial y}) = -gh \frac{\partial z_b}{\partial x} + \frac{\partial}{\rho} (v_t h \frac{\partial U_y^2}{\partial y}) = -gh \frac{\partial z_b}{\partial x} + \frac{\partial}{\rho} (v_t h \frac{\partial U_y^2}{\partial y}) = -gh \frac{\partial z_b}{\partial x} + \frac{\partial}{\rho} (v_t h \frac{\partial U_y^2}{\partial y}) = -gh \frac{\partial z_b}{\partial x} + \frac{\partial}{\rho} (v_t h \frac{\partial U_y^2}{\partial y}) = -gh \frac{\partial z_b}{\partial x} + \frac{\partial}{\rho} (v_t h \frac{\partial U_y^2}{\partial y}) = -gh \frac{\partial z_b}{\partial x} + \frac{\partial}{\rho} (v_t h \frac{\partial U_y^2}{\partial y}) = -gh \frac{\partial z_b}{\partial x} + \frac{\partial}{\rho} (v_t h \frac{\partial U_y^2}{\partial y}) = -gh \frac{\partial z_b}{\partial x} + \frac{\partial}{\rho} (v_t h \frac{\partial U_y^2}{\partial y}) = -gh \frac{\partial z_b}{\partial x} + \frac{\partial}{\rho} (v_t h \frac{\partial U_y^2}{\partial y}) = -gh \frac{\partial z_b}{\partial x} + \frac{\partial}{\rho} (v_t h \frac{\partial U_y^2}{\partial y}) = -gh \frac{\partial z_b}{\partial x} + \frac{\partial}{\rho} (v_t h \frac{\partial U_y^2}{\partial y}) = -gh \frac{\partial z_b}{\partial x} + \frac{\partial}{\rho} (v_t h \frac{\partial U_y^2}{\partial y}) = -gh \frac{\partial z_b}{\partial x} + \frac{\partial}{\rho} (v_t h \frac{\partial U_y^2}{\partial y}) = -gh \frac{\partial z_b}{\partial x} + \frac{\partial}{\rho} (v_t h \frac{\partial U_y^2}{\partial y}) = -gh \frac{\partial z_b}{\partial x} + \frac{\partial}{\rho} (v_t h \frac{\partial U_y^2}{\partial y}) = -gh \frac{\partial z_b}{\partial x} + \frac{\partial}{\rho} (v_t h \frac{\partial U_y^2}{\partial y}) = -gh \frac{\partial U_y^2}{\partial x} + \frac{\partial}{\rho} (v_t h \frac{\partial U_y^2}{\partial y}) = -gh \frac{\partial U_y^2}{\partial x} + \frac{\partial}{\rho} (v_t h \frac{\partial U_y^2}{\partial y}) = -gh \frac{\partial U_y^2}{\partial x} + \frac{\partial}{\rho} (v_t h \frac{\partial U_y^2}{\partial y}) = -gh \frac{\partial U_y^2}{\partial x} + \frac{\partial}{\rho} (v_t h \frac{\partial U_y^2}{\partial y}) = -gh \frac{\partial U_y^2}{\partial x} + \frac{\partial}{\rho} (v_t h \frac{\partial U_y^2}{\partial y}) = -gh \frac{\partial U_y^2}{\partial x} + \frac{\partial}{\rho} (v_t h \frac{\partial U_y^2}{\partial y}) = -gh \frac{\partial U_y^2}{\partial x} + \frac{\partial}{\rho} (v_t h \frac{\partial U_y^2}{\partial y}) = -gh \frac{\partial U_y^2}{\partial x} + \frac{\partial}{\rho} (v_t h \frac{\partial U_y^2}{\partial y}) = -gh \frac{\partial U_y^2}{\partial x} + \frac{\partial}{\rho} ($$

$$\frac{\frac{\partial}{\partial b}(hUy) + \frac{\partial}{\partial x}(hUU) + \frac{\partial}{\partial x}(hUU) + \frac{\partial}{\partial y}(hUU) + \frac{\partial}{\partial y}(hU^2 + g\frac{h^2}{2}) = -gh\frac{\partial Z_b}{\partial y} + \frac{\tau_{s,y}}{\rho} - \frac{\tau_{b,y}}{\rho} + \frac{\partial}{\rho}(yh\frac{\partial U_b}{\partial y}) + \frac{\partial}{\partial y}(yh\frac{\partial U_b}{\partial y}) + \frac{\partial}{\rho}(yh\frac{\partial U_b}{\partial y}) +$$

In general, the method used on Iber for hydraulic modeling to evaluate the flooding scale is based on several essential steps illustrated in the diagram.

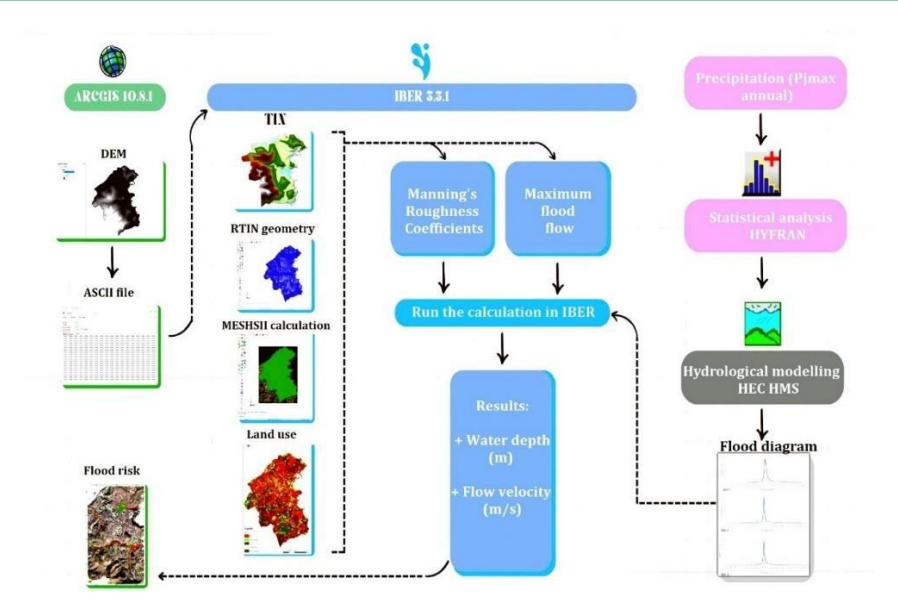


Figure 3: Diagram of the hydrological simulation process in IBER software

The process that follows after data export by Arcgis, is based on several steps and data concluded as follows:

- Input Data: the essential data used for the model is the detailed digital terrain model (DTM), which is converted into ASCII format, the maximum flood flows, and Manning's roughness coefficient based on the types of land use carried out.
- Calculation Modules: Generally, uses 3 main calculation equations
 - The hydrodynamic module, which solves the 2D shallow water equations to determine water depth and velocity.
 - A turbulence module.
 - A sediment transport module.
- Unstructured Mesh: The software works with an unstructured finite-volume mesh, composed of triangular or quadrilateral elements, on which hydraulic variables (water depth, velocity) are calculated at the geometric center of each mesh element.

- Treatment Steps: The methodology is based on three pillars:
 - Pre-processing: import geometry, assign roughness values, create calculation mesh, etc.
 - Processing: Run hydraulic calculations using 2D Saint-Venant equations.
 - Post-processing: Visualize the results obtained, such as flood extent, water depth and flow velocity.
- Boundary Conditions: the return period used is (100), specific peak flow values are assigned for model boundary conditions.
 Furthermore, the water exit was located, and the "supercritical/critical" flow condition was chosen (Bladé et al., 2008; Valentín et al., 2022)
- Maps Obtained: The model can be used to generate various maps of importance to flood risk management. The velocity map and the depth map are of particular interest to us. Land use mapping and classification

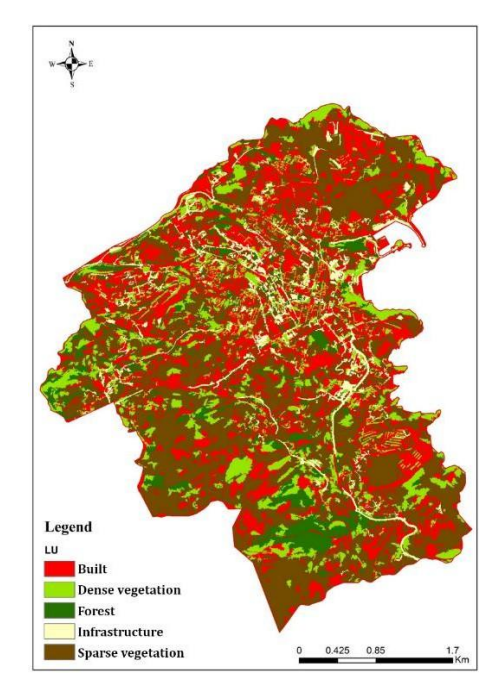


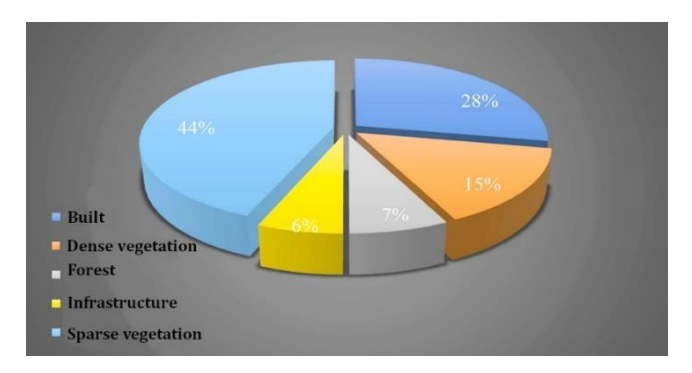
Figure 4: Land use in the catchment area of the city of al Hoceima (Based on satellite image analysis).

Object-oriented classification makes it possible to analyze groups of pixels (objects) in their context, at different scales of landscape perception. This approach considerably improves information extraction capabilities, by enabling the interpreter to rely not only on the spectral values of pixels, but also on morphological parameters such as the size, shape and neighborhood of objects. This enables much richer and more accurate information extraction, particularly for images with very high spatial resolution.

In this study, a land-use map of the city of Al Hoceima was generated using object-oriented classification methodology applied with eCognition software, from a recent satellite image (2024) extracted via Google Earth Pro.

The treatment process in eCognition revolves around four main stages:

- Import and data preparation: This stage involves integrating the 2024 satellite image, ensuring its calibration and preparation for segmentation.
- Segmentation: The aim of this step is to break down the image into homogeneous objects, based on shape and spectral similarity criteria, enabling better differentiation of landscape features.
- Classification: Segmented objects are then classified according to user-defined spectro-morphological and contextual criteria, enabling fine differentiation of land use types.
- Export results: The final result is exported in raster format for further analysis and visualization.



Graph 1: graph of percentages for each land-use classification

Our study area is classified into five categories, based on Manning's roughness values, for integration into the IBER software. These categories reflect the different types of land use, each having a particular impact on runoff and flood risk management.

- Built-up (44%): The built-up class is the most dominant, accounting
 for 44% of the total surface area. With its rugged topography and
 uncontrolled urban expansion, this category represents a major risk
 in terms of flood management. Intensive urbanization reduces
 permeable surfaces, increasing rainwater runoff and the likelihood of
 flooding in densely populated areas. These data are essential for
 assessing the potential impact of flooding on the population and
 infrastructure.
- Dense vegetation (28%): Dense vegetation plays a crucial role in water regulation, facilitating the infiltration of water into the soil and reducing runoff. This vegetation cover acts as a natural barrier against flooding, helping to reduce risks in surrounding areas.
- Forest (7%): Although forest areas cover only 7% of the surface area, they represent an important component in flood prevention. Forests absorb a significant amount of water and stabilize soils, limiting erosion and runoff. These areas therefore play a protective role and deserve to be preserved.

- Infrastructure (6%): Specific infrastructures (such as roads, bridges and industrial facilities) are particularly vulnerable to flooding, especially if they are located in low-lying areas or close to watercourses. Their exposure to flooding can cause major disruption and economic losses. It is therefore essential to take measures to strengthen their resilience.
- Dense vegetation (15%): Dense vegetation is a transition zone where
 infiltration is limited and the soil is more exposed to erosion. In the
 event of intense precipitation, these zones can lead to increased
 runoff and, consequently, a higher risk of flooding. Simulations des
 hydrogrammes de crues

With regard to flood hazard and its management, it is necessary to consider flood discharge as an unforeseen event that can cause damage to a vulnerable area. So, in addition to taking into account the probability of a specific flow, it is essential, for operational purposes, to define the characteristic of the flood, i.e. to derisve from the hydrograms based on the time variable (QTvar) the essential parameters such as the base, rise and fall of the flood, as well as the peak and volume of the flood. (Bhunya et al., 2011) .We define the characteristics as follow (Bouazza, S., 2019):

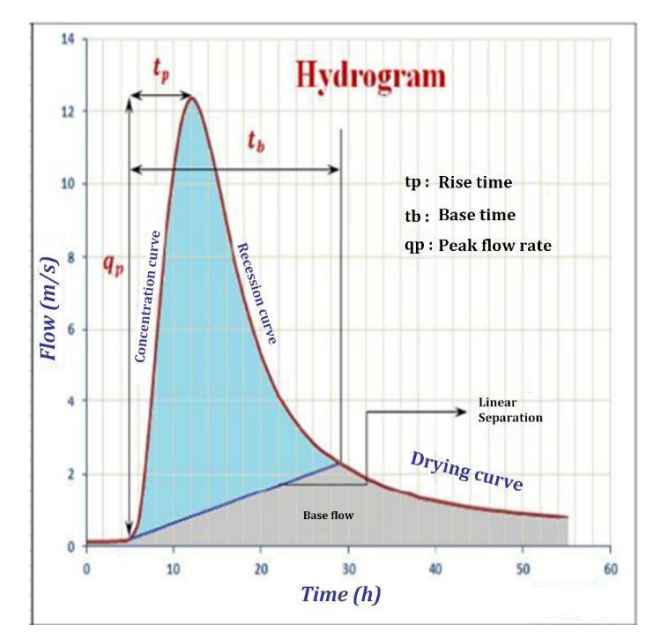


Figure 5: Hydrogram of flood

- Base time: total duration of the flood between two flows not directly influenced by precipitation.
- Rise time: time between the end of the drying phase and the peak flood discharge.
- Descent time: time between flood peak and beginning of drying phase
- Peak flow: maximum instantaneous flow

The Hydrologic Modeling System (HEC-HMS) is a hydrological modeling software created by the Hydrologic Engineering Center of the US Army Corps of Engineers (Unduche, et al., 2018; USACE-HEC, 2016). HEC-HMS employs distinct models to depict each element of the runoff process(Unduche et al., 2018, El Yousfi et al., 2023). The meteorological component is the primary computational unit that spatially and temporally distributes precipitation input over the basin. The precipitation experiences losses as modeled by the precipitation loss component (Cunderlik & Simonovic, 2004; Feldman, 2000)

The HEC-HMS simulations generate hydrographs that illustrate discharge as a function of time, which is crucial for assessing the potential impact of a flood on the watershed. The final result is as follows:

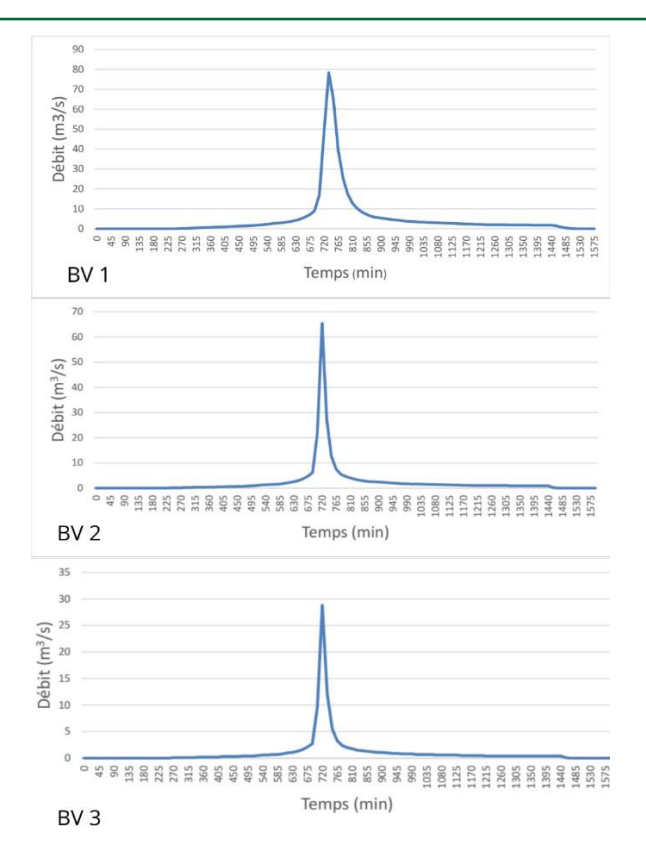


Figure 6: Flood hydrogram for each watershed (BV)

- BV1: The maximum flow rate is around 80 m3/s, indicating a high flood in this catchment area, with a short time of concentration and a rapid flow rate, resulting in significant runoff. This is due to the impermeable soil and the layout of the area, with little vegetation, which allow rapid runoff into the watercourses. This indicates a high risk of flooding in this watershed.
- BV2: The maximum flood discharge is slightly lower than that of BV 1, reaching around 65 m3/s, with a rapid rise, suggesting that the soil is more permeable and covered with denser vegetation, which may
- result in a moderate flood risk.
- BV3: The maximum flow in this basin is lower than in the other two basins, reaching around 30 m3/s. However, it still increases at the same rate, suggesting better infiltration of water into the soil and a more effective buffering effect, due to the pronounced relief.

5. RESULTS

5.1 Speed map

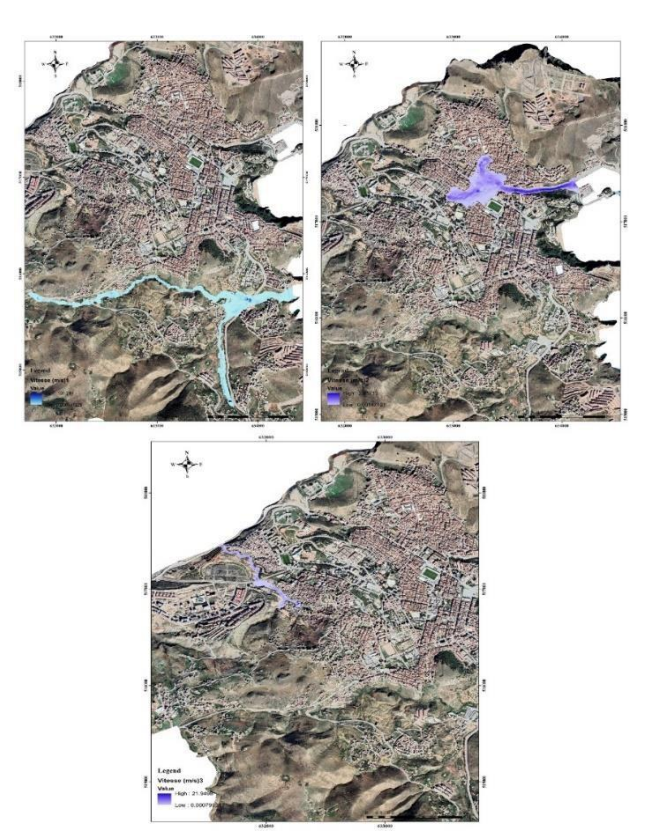


Figure 7: Speed map for each watershed (BV)

5.1.1 First map (Speed 1)

In most of the flood zone, the flow is generally slow. The velocity values shown in the legend range from 0.00094 to 101.218 m/s, reflecting great variability. However, the majority of flooded areas (in light blue) appear to correspond to lower velocities, the low velocity being due to the shape of the basin. Areas with higher velocities are mainly found in areas with slabs and bridges, as this is where the flow is more concentrated.

5.1.2 Second map (Speed 2)

On this map, we see a high concentration of velocities in a part of the watershed towards the right of the map, where flow velocity reaches up to 291.713 m/s. This suggests an area of much faster flow, due to the steep gradient. Velocities are lower in other parts of the area, with areas of water where flow is slowed (light blue areas).

5.1.3 Third map (Speed 3)

In this zone, maximum velocity reaches $21.949\,$ m/s. The velocity distribution reveals areas where flow is more concentrated in certain parts of the river network, as in the dark purple areas. Velocities remain relatively low on the rest of the map, due to less concentrated flow.

5.2 Depth maps

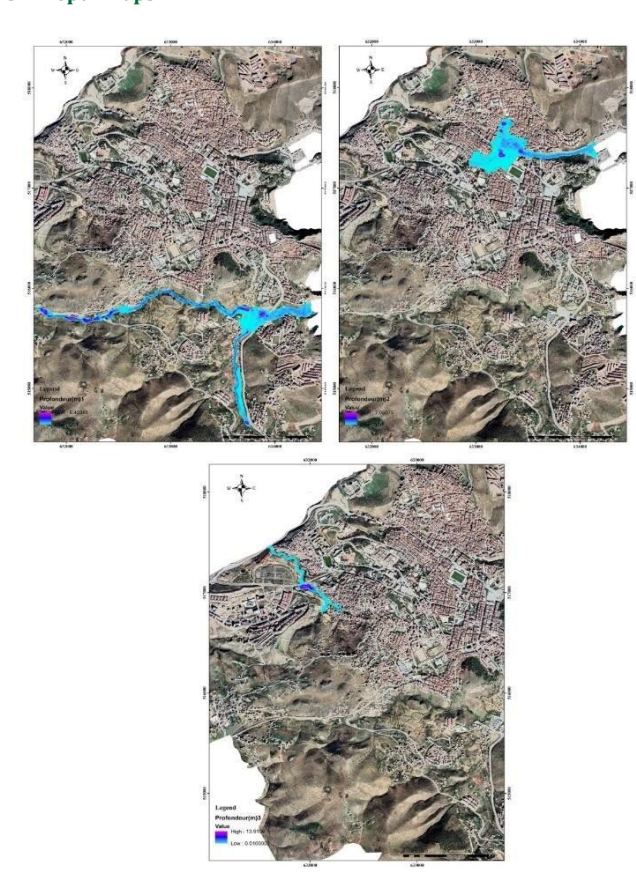


Figure 8: Depth map for each watershed

5.2.1 First map (depth map 1)

According to the legend, the deepest areas can reach a depth of around 6.42 meters, with a purple tint, suggesting a significant accumulation of water. Low-lying areas of the basin show significant water accumulation, increasing the risk to nearby urban infrastructure and housing, which we have uncovered through bridges and embankments.

5.2.2 Second map (depth map 2)

Maximum depths here are around 7.06 metres. This suggests a higher risk of flooding in habitable areas, increasing the danger to residents and the stability of buildings. The widening of the blue zones suggests greater flooding in terms of surface area, probably affecting dense urban infrastructures and roadways.

5.2.3 Third map (depth map 3)

The depth in this case rises to 13.91 meters, suggesting a very significant accumulation of water, which is attributed to a particular topographical configuration (lower part of the Oued)

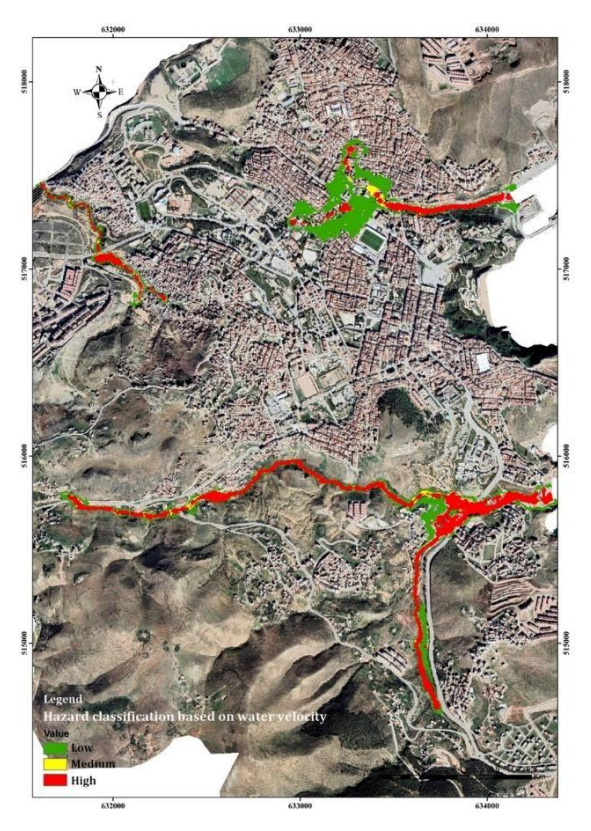


Figure 9: Finale flood risk map for the city of Al Hoceima

The categorization of areas most affected by flooding is an essential factor in assessing the level of hazard by using the Spanish Agència Catalana de l'Aigua (ACA) methodology (Fernandes and Malheiro, 2019; Valentín et al., 2022; Djafri et al., 2024). Figure 9 visually represents the flood-risk areas obtained using the Iber software, incorporating data on water depth and flow velocity. This method allows for a precise assessment of vulnerable areas at various levels of flood risk within the studied urban center. The following analysis is based on a classification of flood risks into three categories: low, medium, and high, based on the hydraulic parameters generated by the simulation.

The map distinguishes three risk levels:

- Low Risk (green): These areas correspond to sectors where water depth and flow velocity are relatively low, indicating a minimal danger level. While these areas may be exposed to potential flooding, the risk to infrastructure and individuals is negligible.
- Medium Risk (yellow): Moderate hazard zones are characterized by water depth or flow velocity values that are relatively low to moderate, but sufficient to cause significant impacts in the event of flooding. These areas present a notable risk of damage, especially to light infrastructure and homes located near watercourses. The presence of this risk level highlights the need for appropriate intervention and management measures.
- High Risk (red): These areas are exposed to high hazards, with maximum water depth and flow velocity values, indicating a significant risk to both people and infrastructure. The likelihood of severe damage is considerable in these sectors, justifying the implementation of special protective measures. These highly vulnerable zones require priority attention in terms of risk management and infrastructure planning.

5.3 Flood risk management

To anticipate the human and material damages caused by floods, it is essential to understand three key aspects: prevention and mitigation, crisis management, and lessons learned. (Tanguy, 2012).

- Prevention and mitigation: This component is based on a detailed understanding of the area, as well as the mapping of risk zones. It provides an overall view to avoid and reduce human and economic vulnerabilities through actions such as protecting existing infrastructure, raising awareness and informing the population, and limiting the development of properties in areas exposed to flood risks. (Hostache & Puech, 2015; Tanguy, 2012).
- Crisis management: It comes into play in emergency situations and involves a critical time constraint. One of the major priorities is to quickly assess the extent of the flooding and locate the most vulnerable populations. The goal is to deploy the most appropriate resources and rescue operations as quickly as possible in order to minimize the human and material consequences of the disaster (Tanguy, 2012). In this situation, it is essential that all stakeholders work in coordination to develop resilience and gradually engage in the field of disaster risk reduction.
- Learned lessons: Also known as the return period, this is the most important component, as it aims to predict damages based on past events, in order to implement proper management at the critical moments to control the threatened territory. This phase is essential for strengthening or adapting risk prevention policies and improving the protection of vulnerable elements in the face of future floods.

5.3.1 Precipitation

Flooding often results from intense or prolonged rainfall that surpasses the infiltration capacity of the soil or overwhelms local drainage systems. The amount and duration of rainfall are crucial factors in flood risk: brief, heavy rains tend to create rapid surface runoff, while sustained, moderate rainfall can saturate the soil over time, leading to slower, gradual flooding. These effects are intensified in areas with steep terrain or urban development, where impermeable surfaces reduce natural infiltration and promote faster runoff. This scenario is a growing concern for water management in urbanized and mountainous regions, where adapted drainage infrastructure and urban planning that incorporates hydrological risks are essential.

Al Hoceima, with its rugged terrain and varied climate, exemplifies this relationship between rainfall and flood risk. The region experiences notable rainfall during the winter months, particularly from November to February, often leading to intense precipitation events. Combined with Al Hoceima's geographical characteristics, these months increase the likelihood of flash floods and rapid runoff toward urban and low-lying areas, exacerbated by insufficient drainage systems, particularly in densely populated zones.

An examination of monthly and annual precipitation data from Station No. 913 in Al Hoceima (coordinates X: 634000, Y: 516800, Z: 40) underscores this seasonal concentration, highlighting winter months as periods of elevated flood risk. The following analysis, illustrated by two types of graphs, underscores the climatic factors that influence flood potential in the region:

6. CONCLUSION

Flood risk is considered one of the most destructive natural phenomena, causing significant human and material losses and disrupting infrastructure at all levels, both locally and internationally. Floods are triggered by a combination of natural factors, such as heavy rainfall, snowmelt, and storm surges, often exacerbated by human activities such as unplanned urbanization and deforestation.

In this context, the objective of this report was to create a flood map for the Al Hoceima region using an appropriate methodology and advanced modeling tools, such as the IBER and HEC-HMS software. The goal was to produce an accurate map of flood-risk areas, taking into account hydrological and topographical parameters, to provide a reliable tool for decision-making and urban planning.

The final flood map highlights the combination of water depth and flow velocity characteristics. It classifies the risk into three levels: low, medium, and high. This tool is essential for land-use planning, enabling local authorities to identify the most exposed areas and plan appropriate interventions. Suggested actions include strengthening infrastructure, limiting urban development in high-risk areas, and implementing early warning systems, along with raising awareness and encouraging community involvement.

Improving resilience to floods requires concerted efforts across several areas, ranging from infrastructure enhancement to community awareness. Effective flood risk management is crucial not only to protect populations and infrastructure but also to promote sustainable economic and social development in the Al Hoceima region. Ultimately, flood-risk mapping is an essential foundation for anticipating and mitigating the impacts of these natural disasters, ensuring a safer and more resilient future for the region and its inhabitants.

REFERENCES

- Adil, J., Chourak, M., Farid, B., Hichame, S., and Aboubakr, C., 2024. Twodimensional flooding model using IBER software case Study: Saidia City North east of Morocco, 03011.
- Afzal, M. A., Ali, S., Nazeer, A., Khan, M. I., Waqas, M., Aslam, R. A., ... Shah, A. N., 2022. Flood Inundation Modeling by Integrating HEC RAS and Satellite Imagery: A Case Study of the Indus River Basin.
- Alfieri, L., Cohen, S., Galantowicz, J., Schumann, G. J., Trigg, M. A., Zsoter, E., ... Salamon, P., 2018. A global network for operational flood risk reduction, 84, 2017, Pp.149–158. https://doi.org/10.1016/j.envsci.2018.03.014
- ARDC., 2009. World Disasters Report Focus on culture and risk.
- Ashley, S. T., and Ashley, W. S., 2008. Flood Fatalities in the United States, 2004, Pp.805–818. https://doi.org/10.1175/2007JAMC1611.1
- Bhunya, P. K., Panda, S. N., and Goel, M. K., 2011. Synthetic Unit Hydrograph Methods: A Critical Review, Pp.1–8.
- Bladé, E., Cea, L., Corestein, G., Escolano, E., Puertas, J., Vázquez-Cendón, E., ... Coll, A. (n.d.). Iber River modelling simulation tool.
- Bladé, E., Dolz, J., Sánchez-Juny, M., and Gómez-Valentín, M., 2008 .

 Preserving Steady-State in One-Dimensional Finite-Volume
 Computations of River Flow, C(September), Pp.1343–1347.
- Bouazza, S., 2019. Les risques hydrologiques d'inondations et la problématique d'aménagement des territoires de piémont : Cas du "dir" de Taghzirt à Zaouit Echiekh, Province de Béni-Méllal, Maroc.
- Case, T., and Bayadh, E., 2023. Assessment of Urban Vulnerability to Flooding Using Multi-Criteria Analysis, 2022. https://doi.org/10.48084/etasr.4828
- Cea, L., and Puertas, J., 2007. Depth Averaged Modelling of Turbulent Shallow Water Flow with Wet-Dry Fronts, 303–341. https://doi.org/10.1007/s11831-007-9009-3
- Chow, V. Te, Maidment, D. R., and Mays, L. W. (n.d.). Hidrologia Aplicada.
- Costabile, P., Barbero, G., Nagy, E. D., Klaudia, N., Petaccia, G., and Costanzo, C., 2024. Predictive capabilities , robustness and limitations of two event-based approaches for lag time estimation in heterogeneous watersheds Predictive capabilities , robustness and limitations of two event-based approaches for lag time estimation in heterogeneous watersheds a. Journal of Hydrology, 642, 131814. https://doi.org/10.1016/j.jhydrol.2024.131814
- Cunderlik, M. J., and Simonovic, P. S., 2004. Calibration, ver- ification and sensitivity analysis of the HEC-HMS hydro- logic model. London, Ontario: Department of Civil and Environmental Engineering, The University of Western Ontario.
- Dasgupta, S., Laplante, B., Murray, S., Wheeler, D., and Laplante, B., 2009. Climate Change and the Future Impacts of Storm-Surge Disasters in Developing Countries Working Paper 182 September 2009.
- Direction of roads., 2015. Adaptation des Routes Au Risque Et Au

- Changement Climatique Au Maroc.
- Djafri, S. A., Cherhabil, S., and Hafnaoui, M. A., 2024. Flood modeling using HEC-RAS 2D and IBER 2D: a comparative study, 24(9), Pp. 3061– 3076. https://doi.org/10.2166/ws.2024.184
- Elhaddaji, A., 2019. Etude De Protection Contre Les Inondations Au Niveau Du Douar Lalla Aariba, Commune De Nfifa, Province De Chichaoua (Maroc) Réalisée.
- El Yousfi, Y., Himi, M., El Ouarghi, H., Aqnouy, M., Benyoussef, S., Gueddari, H., Tahiri, A., 2023. GIS preprocessing for rainfall-runoff modeling using HEC-HMS in Nekkor watershed (Al-Hoceima, Northern Morocco). In E3S Web of Conferences (Vol. 364, p. 01005). EDP Sciences.
- Feldman, A., 2000. Hydrologic modeling system HEC-HMS: technical reference manual. Davis, CA: US Army Corps of Engineers, Hydrologic Engineering Center., (March).
- Fernandes, F., and Malheiro, A., 2019. Advances in Natural Hazards and Hydrological Risks: Meeting the Challenge.
- Gaudiano, G., 2007. Educación y cambio climático: un desafío inexorable.
- Gomes, A., 2018. Hydraulic modeling for the assessment of flood hazard using the Iber software in the Amarante urban center, 18.
- Hassani, F. El, Hattafi, Y., and Lahrach, A., 2021. Water Dynamics of the Sefrou Watershed, Northern Tabular Middle Atlas, Morocco, Pp. 102–130. https://doi.org/10.4236/gep.2021.99007
- Hostache, R., and Puech, C., 2015. Caractérisation spatiale de l'aléa inondation à partir d'images satellites RADAR, 2007. https://doi.org/10.4000/cybergeo.7722
- IRFC., 2003. Synthesis Report on Ten ASEAN Countries Disaster Risks Assessment ASEAN Disaster Risk Management Initiative, (December).
- Jean, E., Mignot, M., Paquier, A., Haider, S., Jean, E., Mignot, M., Modeling, S. H., 2010. Modeling floods in a dense urban area using 2D shallow water equations.
- LASRI, M., 2014. Les inondations menaçant l'agglomération de Fès : Caractérisation du bassin versant, étude du risque et cartographie des dangers.
- Mediero, L., Soriano, E., Oria, P., Bagli, S., Castellarin, A., Garrote, L., Santill, D., 2022. Pluvial flooding: High-resolution stochastic hazard mapping in urban areas by using fast-processing DEM-based algorithms, 608. https://doi.org/10.1016/j.jhydrol.2022.127649

- Nkwunonwo, U. C., Whitworth, M., and Baily, B., 2018. Urban flood modelling combining cellular automata framework with semi-implicit finite difference numerical formulation. Journal of African Earth Sciences. https://doi.org/10.1016/j.jafrearsci.2018.10.016
- Ouzerbane, Z., Boughalem, M., Hmaidi, A. El, Aïfa, T., Ouali, A. El, Najine, A., Wafik, A., 2019. Application of GIS to study the physiographic factors and the water resources in the watersheds of Essaouira , Morocco, 2019(04), Pp.480–489.
- Perdikaris, J., Gharabaghi, B., and Rudra, R., 2018. Reference Time of Concentration Estimation for Ungauged Catchments, 7(2), Pp. 58–73. https://doi.org/10.5539/esr.v7n2p58
- Res, C., and Trenberth, K. E., 2011. Changes in precipitation with climate change, 47, Pp. 123–138. https://doi.org/10.3354/cr00953
- Salas Salinas, M. A., 2014. Obras De Protección Contra Inundaciones.
- Sami, G., Filali, A., and Yahyaoui, H., 2021. Flood Hazard in the City of Chemora (Algeria), (May). https://doi.org/10.30892/auog.311103-835
- Satta, A., Kolker, A. S., and Snoussi, M., 2023. Climate risk assessment of the Tangier-Tetouan-Al Hoceima coastal Region (Morocco), (April), Pp. 1–16. https://doi.org/10.3389/fmars.2023.1176350
- Soto, A., and Malpartida, D., 2016. Modelo De Simulación De La Operación Del Embalse Gallito Ciego Utilizando El Software Iber.
- Tanguy, M., 2012. Cartographie Du Risque D'inondation En Milieu Urbain Adaptée À La Gestion De Crise Analyse Préliminaire.
- Unduche, F., Tolossa, H., Senbeta, D., and Zhu, E., 2018. Evaluation of four hydrological models for operational flood forecasting in a Canadian Prairie watershed. Hydrological Sciences Journal, 63(8), Pp. 1133– 1149. https://doi.org/10.1080/02626667.2018.1474219
- USACE-HEC., 2016. Hydrologic Modeling System HEC-HMS, (August).
- Valentín, J., García, G., Enrique, J., Panta, R., Salvador, D., Reynoso, F., ... Sánchez, R., 2022. river basin Global climate circulation models project more intense temperature and rainfall, 13(71). https://doi.org/10.29298/rmcf.v13i71.1238
- Vignesh, K. S., Anandakumar, I., Ranjan, R., and Borah, D., 2021. Flood vulnerability assessment using an integrated approach of multi criteria decision making model and geospatial techniques. Modeling Earth Systems and Environment, (June). https://doi.org/10.1007/s40808-020-00997-2

